Raman and $^{19}F\{^1H\}$ Nuclear Overhauser Evidence for a Rigid Solution Conformation of *Escherichia coli* 5-Fluorouracil 5S Ribonucleic Acid†

Alan G. Marshall* and James L. Smith‡

ABSTRACT: *Escherichia coli* cells grown on a medium containing 5-fluorouracil (FU) produce 5S RNA whose uracil residues are ~80% replaced by FU. The Raman spectra of native and FU–5S RNA are very similar, confirming similar solution conformations for the two species and a highly base-stacked structure in solution. The 254-MHz ^{19}F NMR spectrum of FU-5S RNA shows that the 20-odd FU residues reside in at least ten distinct chemical environments, suggesting a highly ordered structure. Comparison of theoretical and experimental $^{19}F\{^1H\}$ nuclear Overhauser enhancements demonstrates definitively that virtually all the labeled uracils are bound to a rigid macromolecular frame, with a rotational correlation time of about 10 ns or longer. Since these uracils are widely distributed throughout the nucleotide primary sequence, it may be concluded that the entire FU–5S RNA solution structure is relatively rigid, in agreement with the most recently proposed "cloverleaf" secondary structural model for native prokaryotic 5S RNA.

The structure and function of prokaryotic 5S RNA have recently been reviewed (Erdmann et al., 1979). Prokaryotic 5S RNA is thought to help anchor transfer RNA to the aminoacyl ("A") site on the large ribosomal subunit during protein synthesis. The *function* of 5S RNA is largely conserved between different prokaryotic species because 5S RNA from one species can be reconstituted with the remaining ribosomal components from another species to give an active ribosome (Bellemare et al., 1975; Delihas et al., 1975). Thus, *structural* information about 5S RNA from any given prokaryotic species should apply generally to other species.

Although the "cloverleaf" secondary structure of tRNA was universally accepted almost immediately after the primary nucleotide sequence had been determined (Holley et al., 1965), literally dozens of secondary structures have been proposed for 5S RNA on the basis of partial enzymatic cleavage patterns, chemical modification of exposed bases, oligoribonucleotide binding to complementary segments of the RNA, UV-visible hypochromism, circular dichroism, low-angle X-ray scattering, and nuclear magnetic resonance spectroscopy (Erdmann, 1976; Erdmann et al., 1979). However, the only secondary structural model consistent with recent Raman (Luoma & Marshall, 1978a; Chen et al., 1978), IR (Appel et al., 1979), 360-MHz ^1H NMR (Luoma et al., 1980), and 400-MHz ^1H NMR (Burns et al., 1980) results is the modified "cloverleaf" shown in Figure 1, first proposed in 1978 (Luoma & Marshall, 1978a,b). This model is distinguished from virtually all previously proposed 5S RNA secondary structures in having a very high degree of base pairing. For example, 65% of the uracils are base paired in the structure of Figure 1 compared to only 40% in a popular previous model (Fox & Woese, 1975). Moreover, 400-MHz ^1H NMR results (Burns et al., 1980) show at least 31 base pairs for *Escherichia coli* 5S RNA in solution compared to 37 and 23 in the Luoma–Marshall and Fox–Woese models.

The uracil residues of *E. coli* tRNA and 5S RNA can be replaced by FU without significant change in function, as judged by FU–5S RNA binding to ribosomes (Johnson et al., 1969) and tRNA amino acid acceptor function (Kaiser, 1969), optical spectrum (Kaiser, 1969), or heat denaturation profile (Horowitz et al., 1974). The optical melting profile for FU–5S RNA from *E. coli* has the same T_m and only slightly smaller hypochromism than that of native 5S RNA (I. I. Kaiser, private communication of unpublished results). Structural conclusions from FU–5S RNA should thus apply to native 5S RNA as well.

The very high percent incorporation of FU in place of normal uracil or uracil-derived residues in tRNA [90.7% (Kaiser & Young, 1975) and 93% (Horowitz et al., 1977)] strongly suggests that FU substitutes randomly for uracil in RNA primary sequences. Fluorine was first introduced as a nuclear spin-label in RNA in 1977 (Marshall & Smith, 1977) for *E. coli* 5S RNA and subsequently independently for $tRNA_1^{Val}$ (Horowitz et al., 1977). The large number of resolved peaks in FU–5S RNA and FU-$tRNA_1^{Val}$ suggests a well-ordered solution structure since the ^{19}F NMR spectrum of FU–5S RNA or FU-tRNA collapses to a single peak (i.e., a common chemical environment) for all the FU residues on heating to 75 °C.

In this paper, we present theoretical calculations of the nuclear Overhauser enhancement (NOE) expected for the ^{19}F NMR signal of 5-fluorouracil in the presence of saturating irradiation of the corresponding proton NMR spectrum. This enhancement turns out to be extraordinarily sensitive to small increases in motional flexibility at the fluorinated residues of a macromolecule the size of 5S RNA (mol wt ≃40 000). The present 254-MHz $^{19}F\{^1H\}$ NOE experiments give a simultaneous measure of flexibility at each of the ~20 different fluorinated uracil residues distributed throughout the nucleotide sequence of *E. coli* FU–5S RNA and thus offer a rather direct means for evaluating proposed secondary structural models for prokaryotic 5S RNA.

Experimental Procedures

Production and Isolation of E. coli FU–5S RNA. *E. coli* B cells were grown on a chemically defined minimal medium (Demerec & Cahn, 1953) at 37 °C. 5-Fluorouracil was added (25 mg/L) in early exponential growth, and the cells were

† From the Departments of Chemistry and Biochemistry, The Ohio State University, Columbus, Ohio 43210. *Received November 16, 1979; revised manuscript received July 29, 1980.* This work was supported by grants (to A.G.M.) from the Natural Sciences and Engineering Research Council of Canada (A-6178), the University of British Columbia (21-9879), and the Alfred P. Sloan Foundation.

* Address correspondence to this author. He is an Alfred P. Sloan Research Fellow, 1976–1980.

‡ Present address: Seattle Metro, Seattle, WA 98119.

0006-2960/80/0419-5955$01.00/0

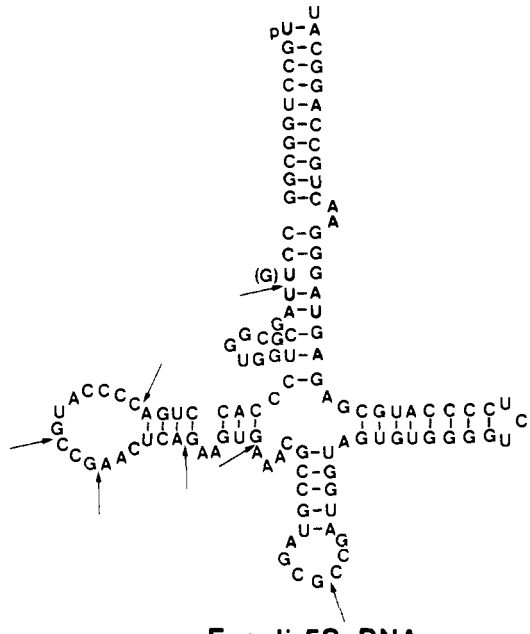

FIGURE 1: Recently proposed cloverleaf secondary structure for *E. coli* 5S RNA. Points of enzymatic partial cleavage are shown by arrows. [Adapted from Luoma & Marshall, 1978a.]

harvested with a Sharples centrifuge following 3 h of agitation and aeration of the culture. Harvested cells were washed twice with 0.01 M Tris-HCl (pH 7.4) containing 10 mM magnesium acetate and stored at −20 °C. In addition to locally grown cells, 2 pounds of FU-treated *E. coli* B cells were graciously provided by Professor I. Kaiser.

RNA was extracted by using equal volumes of water and phenol, centrifuged, and precipitated at −20 °C with 2.5 volumes of 95% ethanol. The soluble RNA was dissolved in 0.3 M NaCl, applied to a DEAE-cellulose anion-exchange column, and eluted with 1 M NaCl. Following reprecipitation with −20 °C ethanol, the RNA's of different sizes were separated by gel-filtration chromatography twice on Sephadex G-75, and the 5S RNA fractions were pooled, precipitated with ethanol, desalted on Sephadex G-25, and lyophilized.

The native (i.e., unfluorinated) 5S RNA and FU–5S RNA were separated by using DEAE-cellulose chromatography (Kaiser, 1969, 1970) on the basis of difference in pK_a for FU (8.15) compared to normal uracil (9.45). This procedure produces 5S RNA in which ~83% of the normal uracil is replaced by FU, as confirmed by radioactive counting of similar preparations with FU labeled with carbon-14 at the C-2 position.

Polyacrylamide gel electrophoresis by the method of Rubin (Rubin, 1973) indicated that the FU–5S RNA was more than 95% homogeneous, with a trace of transfer RNA.

^{19}F Nuclear Magnetic Resonance Spectroscopy. Lyophilized FU–5S RNA was dissolved in D_2O buffer, pH 7.0, containing 10 mM phosphate, 10 mM $MgCl_2$, and 100 mM NaCl. Sample concentration of RNA was determined by A_{260} measurement on the basis of 21 A_{260} units per mg per mL of 5S RNA (Litt, 1968).

^{19}F NMR measurements were obtained by using a Bruker WH-270 NMR spectrometer operating at 254 MHz at the Biochemistry Department, University of Alberta, with the kind help of Professor B. D. Sykes. Typical experimental parameters included 8K time-domain data set, 5000 Hz spectral width, 0.5-s relaxation delay, quadrature detection, 10-μs pulse width ~90°), and signal-to-noise enhancement by exponential multiplication to give a line broadening of 5 Hz. Overhauser experiments were based on broad-band decoupling of the proton spectrum at 270 MHz, with the decoupling frequency set either on- (NOE present) or off-resonance (NOE absent). Since gated decoupling was not used, the NOE spectrum is Overhauser enhanced but not decoupled. Thus, any ^{19}F intensity changes on proton irradiation are due only to Overhauser effects and not to collapse of the F–H scalar coupling. T_1 measurements were performed by the usual inversion–recovery (180°–τ–90°) sequence.

Raman Spectra. Aqueous (or D_2O) samples were prepared with deionized water containing 50 mM $NaClO_4$ as an internal Raman frequency and intensity standard. Raman samples consisted of 20-μL aliquots in Kimax melting point capillary tubes (0.8–1.1 mm i.d.). Spectra were obtained with a Spex Ramalog 4 laser Raman system equipped with a Spectra-Physics Model 164 argon ion laser (5145 Å) by using 600 mW laser power, a spectral slit width of 7–8 cm^{-1}, and a scan speed of 0.2 $cm^{-1}s^{-1}$ with a period of 10 s in pen response. Line positions were determined relative to the 932-cm^{-1} line of $NaClO_4$.

Theory

Nuclear magnetic relaxation time constants, T_1 and T_2, can be used to compute rotational correlation time for a nuclear spin at a given macromolecular site, provided that the relaxation mechanisms are known. For an aromatic fluorine bound to a macromolecule, the principal ^{19}F relaxation pathways depend on ^{19}F–^1H dipole–dipole and ^{19}F chemical shift anisotropy interactions. Separation of the relative contributions of these two interactions to T_2 relaxation requires experiments at two or more applied magnetic fields and an experimental ^{19}F spectrum in which the component peaks are well resolved. These requirements are satisfied for the *E. coli* fluorotyrosine alkaline phosphatase system, for which the elegant ^{19}F NMR experiments of Hull and Sykes have produced a wealth of detailed structural and motional information about individual fluorotyrosine residues (Sykes et al., 1974; Hull & Sykes, 1974–1976).

The situation is much simpler for T_1, however, because the chemical shift anisotropy mechanism contributes negligibly to ^{19}F T_1 relaxation for *m*-fluorotyrosine (Hull & Sykes, 1975) or 5-fluorouracil (whose geometry and ^{19}F relaxation are very similar to those of *m*-fluorotyrosine). Thus, the ^{19}F T_1 value may be computed from the dipole–dipole interaction alone, whose strength varies as r^{-6}, where r is the internuclear distance between the ^{19}F and the ^1H nucleus to which it is dipole coupled. For 5-fluorouracil, the dipole–dipole interaction should thus be dominated by intramolecular coupling to the nearest (H-6) proton, for which r is readily computed to be 2.58 Å from the known X-ray crystal structure (Veot & Rich, 1969; Fallow, 1973).

Although rotational motional information can be obtained from direct measurement of T_1, such measurements are time consuming and are relatively inaccurate when (as in this case) the ^{19}F spectrum consists of incompletely resolved peaks. A particularly simple and rapid T_1 determination is via the nuclear Overhauser experiment, in which the "I" spin (^{19}F) is observed as usual in W_0. presence or absence of saturation of the "S" (^1H) spin transitions using strong irradiation at the proton NMR frequency. Under these conditions, an NOE "enhancement," $f_I(S)$, can be computed from the ^{19}F peak area in the presence or absence of proton irradiation (Noggle & Schirmer, 1971):

$$f_I(S) = {}^{19}F \text{ area (with } {}^1H \text{ irradiation)} - {}^{19}F \text{ area (without } {}^1H \text{ irradiation)}/{}^{19}F \text{ area (no } {}^1H \text{ irradiation)} \quad (1)$$

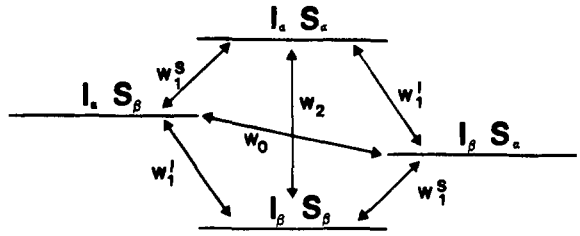

FIGURE 2: Energy levels and transition rates (W) for a system of two unlike nuclei, I (^{19}F) and S (^{1}H), of spin $^1/_2$. The W subscripts refer to zero-, single-, and double-quantum transitions (see text).

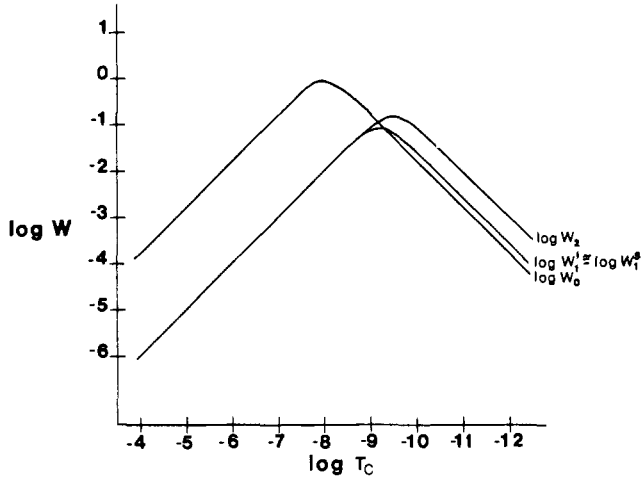

FIGURE 3: Log–plot of transition rates vs. rotational correlation time for the system of Figure 2, in which I is F-5 and S is H-6 of 5-fluorouracil. ^{19}F relaxation is taken as pure dipolar between F-5 and H-6, resulting from isotropic rotational diffusion.

The NOE for a system of two half-integral spins (I = ^{19}F; S = ^{1}H) is given by eq 2, in which the transition rates, W_i,

$$f_I(S) = \frac{W_2 - W_0}{2W_1^I + W_0 + W_2} \quad (2)$$

are defined in Figure 2. The magnitude and sign of the enhancement clearly depend on the relative magnitudes of the double-quantum transition rate, W_2, and the zero-quantum transition rate, W_0.

Figure 3 shows the variation of W_0, W_1^I, and W_2 with rotational correlation time for isotropic rotational diffusion of 5-fluorouracil, assuming intramolecular dipole–dipole interaction between the F-5 and H-6 proton, calculated for an external magnetic field strength of 6.34 T (254-MHz ^{19}F Larmor frequency; 270-MHz ^{1}H Larmor frequency) by using Solomon's equations for dipole–dipole coupling of unlike half-integral spins (Solomon, 1955):

$$W_0 = 1.633 \times 10^8 \frac{\tau_{rot}}{1 + (\omega_I - \omega_S)^2\tau_{rot}^2} \text{ s}^{-1} \quad (3)$$

$$W_1^I = 2.45 \times 10^8 \frac{\tau_{rot}}{1 + \omega_I^2\tau_{rot}^2} \text{ s}^{-1} \quad (4)$$

$$W_2 = 9.80 \times 10^8 \frac{\tau_{rot}}{1 + (\omega_I + \omega_S)\tau_{rot}^2} \text{ s}^{-1} \quad (5)$$

in which τ_{rot} is the rotational correlation time; $\omega_I = (2\pi)(254 \times 10^6)$ rad s^{-1} and $\omega_S = (2\pi)270 \times 10^6$ rad s^{-1} are the Larmor frequencies of ^{19}F and ^{1}H at this magnetic field strength, r_{F-H} = 2.58 Å.

The fractional Overhauser enhancement, $f_I(S)$, is readily calculated from the transition rates plotted in Figure 3 and

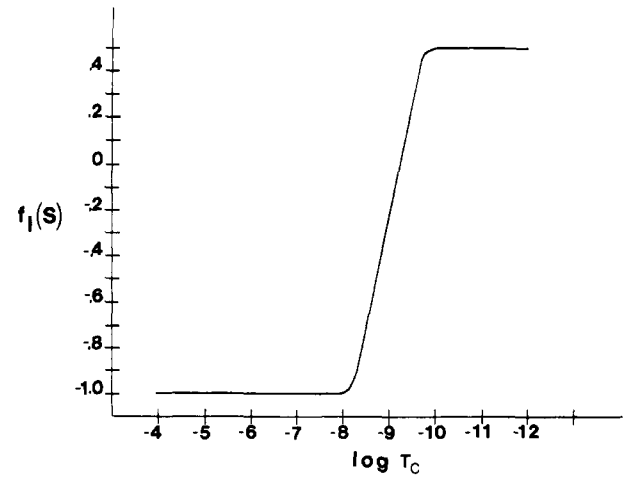

FIGURE 4: ^{19}F{^{1}H} fractional nuclear Overhauser enhancement factor vs. rotational correlation time (log scale) for 5-fluorouracil, computed from the transition rates of Figure 3 (see text).

is displayed as a function of τ_{rot} in Figure 4. As initially noted by Balaram et al. (1972) for a similar problem, a sufficiently long τ_{rot} ($\leq$10 ns in this case) leads to a negative "enhancement" of −1 so that the ^{19}F signal *disappears entirely* when the H-6 proton is irradiated. Furthermore, as rotational diffusion increases to τ_{rot} values less than 10 ns W_2 becomes larger than W_0 and $f_I(S)$ passes rapidly through zero to approach the fast-motion limit of +0.5 (i.e., the ^{19}F signal is 1.5 times *larger* when the H-6 proton is irradiated).

If FU–5S RNA were a rigid sphere, its τ_{rot} calculated from the Stokes–Einstein equation (Marshall, 1978)

$$\tau_{rot} = 4\pi\eta R^3/(3kT) \quad (6)$$

in which η is viscosity, k is Boltzmann's constant, T is absolute temperature, and R is the macromolecular radius (computed from the molecular weight of 40 000) would be about 10 ns, assuming no water of hydration. A rigid FU/5S RNA should thus exhibit $f_I(S) = -1$ (see Figure 4), corresponding to complete nulling of the ^{19}F signal on irradiation of the H-6 proton. However, because of the marked variation of $f_I(S)$ with τ_{rot} in this motional region, even a small increase in local flexibility at the labeled site should lead to a large increase in $f_I(S)$ and an incomplete nulling (or even increase) of the ^{19}F peak on proton irradiation. Thus, the instrumental and molecular parameters of the FU–5S RNA Overhauser experiment happen to fall in a range such that the NOE experiment is optimally tuned to detect local flexibility at the labeled uracils of FU–5S RNA.

Results and Discussion

Raman Spectra. Virtually all the peaks in the Raman spectra of dUrd and 5FdUrd in Figure 5 may be assigned by comparison to the very similar spectrum of Urd (Lord & Thomas, 1967). The principal effects of fluorination are the following: (i) the two carbonyl stretch frequencies in 5FdUrd are equal (1676 cm^{-1}), presumably because the C_4=O frequency has increased relative to dUrd [α-Fluoro substitution is known to shift Raman carbonyl stretching to higher frequency in model compounds (Bellamy, 1975).] and (ii) the new prominent peak at 1362 cm^{-1} in 5FdUrd, which is assigned by us as a C–F stretch because the peak is relatively unchanged on going from H_2O to D_2O and because C–F stretch frequencies have been reported in this region (Dollish et al., 1974).

The 1100-cm^{-1} (PO_2^- stretch) Raman peak intensity is relatively independent of RNA conformation at a given ionic

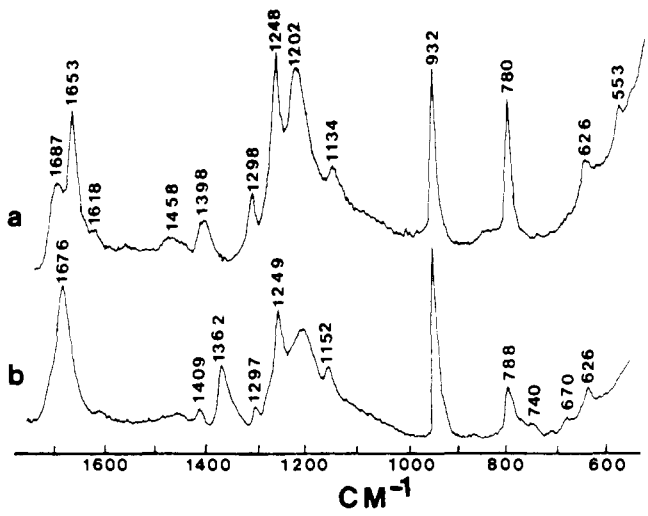

FIGURE 5: Laser Raman spectra of neutral dUrd and 5FdUrd in D_2O containing 50 mM $NaClO_4$. (a) 50 mM dUrd, pH 6.2; (b) 50 mM 5FdUrd, pH 5.8.

Table I: Relative Peak Heights in the Raman Spectra of Figure 8[a]

frequency (cm^{-1})	assignment	5S RNA	FU-5S RNA
670	G	0.66	0.70
725	A	0.65	0.74
785	C,U	2.21	2.10
814	-COPOC-	1.65	1.73
1100	PO_2^-	1.00	1.00
1242	U,C,A	1.17	1.16
1321	G	1.31	1.36
1338	A	1.04	1.10
1485	A,G	2.21	2.06
1575	A,G	1.94	2.03

[a] All heights have been scaled to the height of the 1100-cm^{-1} peak as 1.00.

strength (Chen et al., 1978). The intensities of the remaining peaks, scaled to the 1100-cm^{-1} intensity, have been shown to give an accurate measure of base-stacking for guanosine (670 cm^{-1}) and adenosine (725 cm^{-1}) residues as well as a measure of A-helix content (814 cm^{-1}) (Luoma & Marshall, 1978a,b; Chen et al., 1978). The great similarities in peak intensities (as determined from peak heights) for normal and FU-5S RNA Raman spectra (Figure 6 and Table I) suggest highly similar solution conformations for FU-5S RNA and normal 5S RNA from *E. coli*. The observed differences can in fact be ascribed largely to intrinsic Raman intensity differences between dUrd and 5FdUrd (figure 5). For example, the 782-cm^{-1} line of dUrd (in H_2O, not shown) decreases ~40% upon 5-fluorination. The 2.21 peak height at 785 cm^{-1} in native 5S RNA is a sum of 0.55 (uridine, 25%) and 1.66 (cytidine, 75%); thus, an 80% replacement of Urd by 5FUrd in *E. coli* 5S RNA would be expected to reduce the 785-cm^{-1} peak height by about 11%, compared to the observed reduction of about 5%. The remaining discrepancy may result from altered hypochromic effects due to altered stacking interactions between FUrd and neighboring bases.

^{19}F NMR. Figure 7 shows the 254-MHz ^{19}F NMR spectrum of FU-5S RNA. At least ten different chemical shifts (corresponding to ten distinct chemical environments) are now resolved, in contrast to only four groups of peaks in our preliminary 94.1-MHz results (Marshall & Smith, 1977). Peaks 5 and 6 have the same chemical shift as the single peak obtained on heat denaturation; thus, this part of the spectrum probably corresponds to FU residues exposed to solution. In support of this view, it may be noted that peaks 5 and 6 are

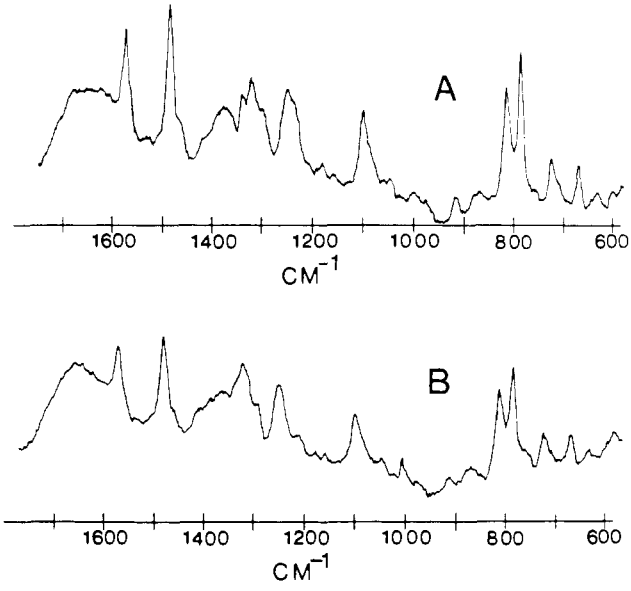

FIGURE 6: Laser Raman spectra in H_2O. (a) *E. coli* 5S RNA; (b) *E. coli* FU-5S RNA. Buffer included 0.01 M phosphate, pH adjusted to 7.0, 100 mM NaCl, and 10 mM $MgCl_2$. RNA concentrations were ~1 mM.

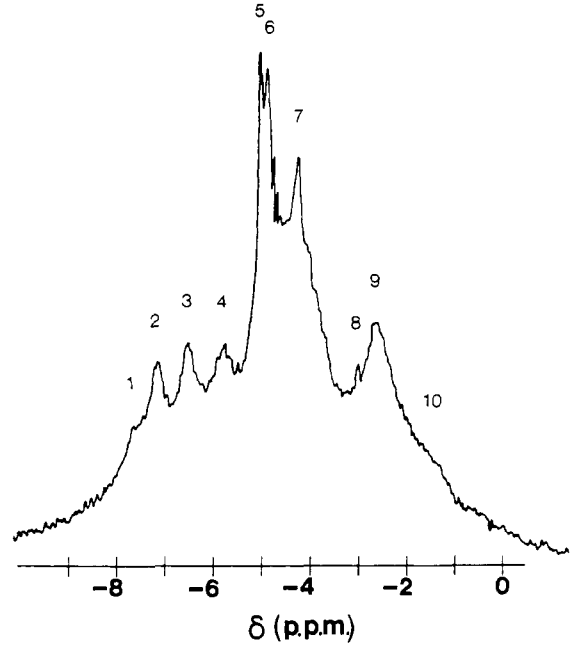

FIGURE 7: ^{19}F nuclear magnetic resonance spectrum (254 MHz) of FU-5S RNA. The spectrum was obtained from Fourier transformation of the free induction decay accumulated from 38 000 time-domain transients (5-mm sample) according to the parameters listed under Experimental Procedures. Chemical shifts are measured with respect to 5-fluorouracil.

much narrower than the peaks shifted to either side and therfore correspond to residues that are more rotationally labile than the shifted (and presumably "buried") peaks. Furthermore, T_1 measurements indicated that virtually all the observed peaks have relatively short T_1 (~0.3 s), in agreement with the (minimum) T_1 calculated to occur for τ_{rot} = 10 ns (corresponding to a rigid solution structure).

The $^{19}F\{^1H\}$ NOE experimental results of Figure 8 are particularly striking. It is clear that virtually the entire ^{19}F spectrum is completely nulled on ^1H irradiation, definitely confirming (see Figure 4) that essentially all the fluorinated uracil residues have rotational correlation times approaching 10 ns or longer. Furthermore, demonstration of the full Ov-

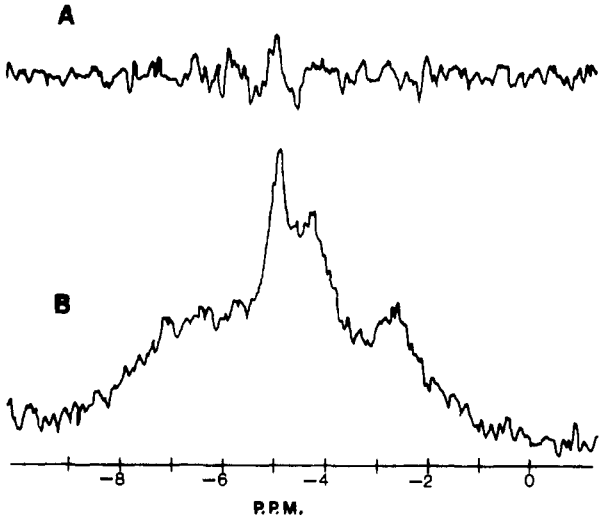

FIGURE 8: ^{19}F NMR spectra (254 MHz) of FU-5S RNA. (A) ^{19}F spectrum (from 1000 transients) obtained immediately following broad-band saturating irradiation of the corresponding ^1H NMR spectrum. The decoupling oscillator was turned off during ^{19}F data acquisition. (B) ^{19}F spectrum (from 1000 transients) for the same system but in the absence of irradiation at the ^1H-resonant frequencies.

erhauser nulling of the ^{19}F resonances [$f_I(S) = -1$] confirms that T_1 relaxation is pure dipolar, as assumed in the theoretical calculations (cf. Hull & Sykes, 1975). [Strictly speaking, the $f_I(S) = -1$ result can also occur in the presence of very rapid internal rotations (Hull & Sykes, 1975). However, such rapid internal motion would have the additional effect of narrowing the ^{19}F resonances to line widths less than are observed in Figure 7. Thus, we may safely conclude that the τ_{rot} values are, in fact, very long (10 ns or greater) rather than very short.]

Summary

In virtually all previously proposed secondary structural models for prokaryotic 5S RNA (Erdmann, 1976; Erdmann et al., 1979; Appel et al., 1979), a large fraction (usually more than half) of the uracils are left unpaired. In contrast, the present theoretical and experimental ^{19}F NMR and $^{19}F\{^1H\}$ nuclear Overhauser enhancement results convincingly demonstrate that essentially all of the fluorouracil residues in *E. coli* FU-5S RNA are bound firmly to a rigid macromolecular frame in solution. Moreover, the present Raman data indicate that the fluorinated and normal *E. coli* 5S RNA exhibit very similar base-stacking properties in solution and thus probably have very similar conformations. These results are thus consistent with recent Raman data (Chen et al., 1978; Smith, 1979) showing a high degree of overall base-pairing and RNA A-helix content and with our own recent (Burns et al., 1980) 400-MHz ^1H NMR spectra and simulations showing at least 31 base pairs for *E. coli* 5S RNA. Taken together, these data all lend strong support to the most recently proposed "cloverleaf" secondary structure (Figure 1) for prokaryotic 5S RNA (Luoma & Marshall, 1978a,b). That model also gave the best simulation of all models tested in recent attempts to fit experimental IR spectra of *E. coli* 5S RNA (Appel et al., 1979).

Acknowledgments

We thank Professor Brian D. Sykes for providing facilities and help in obtaining 254-MHz ^{19}F spectra and Professor Ivan I. Kaiser for a generous gift of *E. coli* B cells grown on FU-containing medium. Professor Gordon Tener and Dr. Greg A. Luoma are thanked for helpful discussions.

References

Appel, B., Erdmann, V. A., Stulz, J., & Ackermann, Th. (1979) *Nucleic Acids Res. 7*, 1043–1057.

Balaram, A., Bothner-by, A., & Dadok, J. (1972) *J. Am. Chem. Soc. 94*, 4015.

Bellamy, L. J. (1975) in *The Infra-Red Spectra of Complex Molecules*, 3rd ed., pp 157–519, Chapman & Hall, London.

Bellemare, G., Vigne, R., & Jordan, B. R. (1975) *Biochimie 55*, 29.

Burns, P. D., Luoma, G. A., & Marshall, A. G. (1980) *Biochem. Biophys. Res. Commun. 96*, 805–811.

Chen, M. C., Giege, R., Lord, R. C., & Rich, A. (1978) *Biochemistry 17*, 3134.

Delihas, N., Dunn, J. J., & Erdmann, V. A. (1975) *FEBS Lett. 58*, 76.

Demerec, M., & Cahn, E. (1953) *J. Bacteriol. 65*, 27.

Dollish, F. U., Fateley, W. A., & Bentley, F. F. (1974) in *Characteristic Raman Frequencies of Organic Compounds*, pp 67–68, Wiley, New York, NY.

Erdmann, V. A. (1976) *Prog. Nucleic Acid Res. Mol. Biol. 18*, 45.

Erdmann, V. A., Appel, B., Digweed, M., Luwe, D., Lorenz, S., Luck, A., Schreiber, A., & Schuster, L. (1979) in *The Genetic and Evolutionary Aspects of Transcriptional and Translational Apparatus*, Kondansha Scientific, Tokyo, Japan.

Fallon, L. (1973) *Acta Crystallogr., Sect. B B59*, 2549.

Fox, G. E., & Woese, C. R. (1975) *Nature (London) 256*, 505.

Holley, R. W., Apgar, J., Everett, G. A., Madison, J. T., Marquisee, M., Merrill, S. H., Penswick, J. R., & Zamir, A. (1965) *Science (Washington, D.C.) 147*, 1462.

Horowitz, J., Ou, C.-N., Ishaq, M., Ofengand, J., & Bierbaum, J. (1974) *J. Mol. Biol. 88*, 301.

Horowitz, J., Ofengand, J., Daniel, W. E., Jr., & Cohn, M. (1977) *J. Biol. Chem. 252*, 4418–4420.

Hull, W. E., & Sykes, B. D. (1974) *Biochemistry 13*, 3431.

Hull, W. E., & Sykes, B. D. (1975) *J. Mol. Biol. 98*, 121.

Hull, W. E., & Sykes, B. D. (1976) *Biochemistry 15*, 1535.

Johnson, J. L., Yamamoto, K. R., Weislogel, P. O., & Horowitz, J. (1969) *Biochemistry 8*, 1901.

Kaiser, I. I. (1969) *Biochemistry 8*, 231.

Kaiser, I. I. (1970) *Biochemistry 9*, 569.

Kaiser, I. I., & Young, P. A. (1975) *J. Chromatogr. 111*, 242–245.

Litt, M. (1968) *Biochem. Biophys. Res. Commun. 32*, 506.

Lord, R. C., & Thomas, G. J. (1967) *Spectrochim. Acta, Part A 23A*, 2551–2591.

Luoma, G. A., & Marshall, A. G. (1978a) *Proc. Natl. Acad. Sci. U.S.A. 75*, 4901.

Luoma, G. A., & Marshall, A. G. (1978b) *J. Mol. Biol. 125*, 95.

Marshall, A. G. (1978) in *Biophysical Chemistry*, p 719, Wiley, New York.

Marshall, A. G., & Smith, J. L. (1977) *J. Am. Chem. Soc. 99*, 635.

Noggle, J. H., & Schirmer, R. E. (1971) in *The Nuclear Overhauser Effect*, Academic Press, New York.

Rubin, G. M. (1973) *J. Biol. Chem. 248*, 3860.

Smith, J. L. (1979) Ph.D. Dissertation, University of British Columbia.

Solomon, I. (1955) *Phys. Rev. 99*, 559.

Sykes, B. D., Weingarten, H. I., & Schlesinger, M. J. (1974) *Proc. Natl. Acad. Sci. U.S.A. 71*, 469.

Veot, D., & Rich, A. (1969) *J. Am. Chem. Soc. 91*, 3069.